Supporting Information

Biomass–Derived Porous Fe_3C/WC/GC Nanocomposite for Efficient Electrocatalysis of Oxygen Reduction

Ming Ma[a], Shijie You[a,*], Wei Wang[a], Guoshuai Liu[a], Dianpeng Qi[b], Xiaodong Chen[b], Jiuhui Qu[c], and Nanqi Ren[a]

[a] State Key Laboratory of Urban Water Resource and Environment, Harbin Institute of Technology, 73 Huanghe Road, Nangang District, Harbin, 150090, P. R. China

[b] School of Materials Science and Engineering, Nanyang Technological University, 50 Nanyang Avenue, 639798, Singapore

[c] State Key Laboratory of Environmental Aquatic Chemistry, Research Center for Eco–Environmental Sciences, Chinese Academy of Sciences, Beijing, 200085, P. R. China

*Corresponding author: E–mail: sjyou@hit.edu.cn; phone: (+86) 451 86282008; fax: (+86) 451 86282110

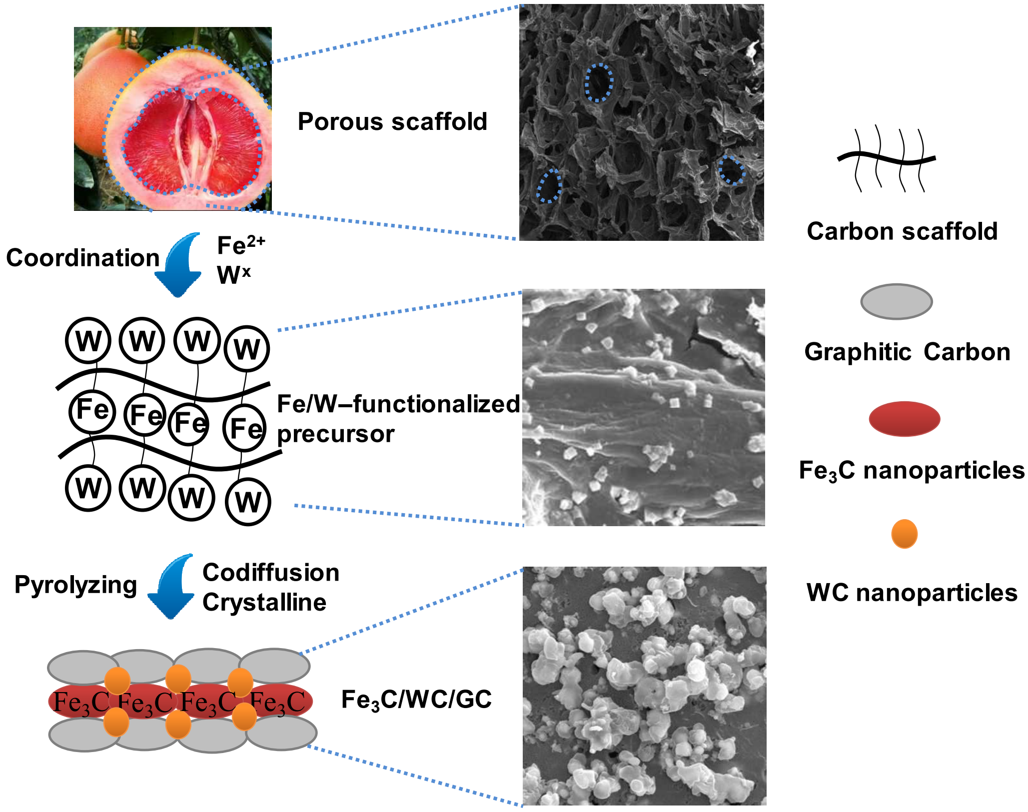

Scheme S1. Schematic illustration of synthesis procedure of Fe_3C/WC/GC composite.

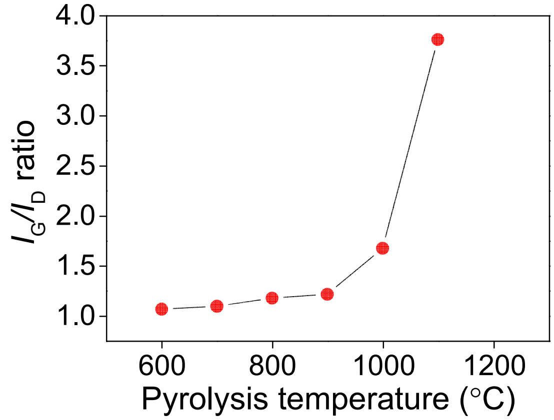

Figure S1. I_G/I_D ratio as function of pyrolysis temperature, derived from Figure 1b.

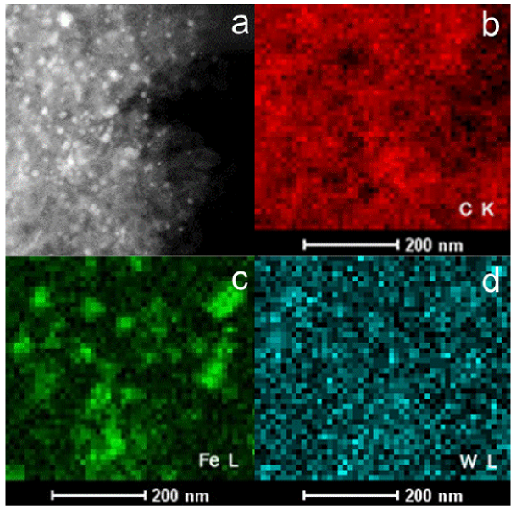

Figure S2. (a) STEM and corresponding MAPPING images of (b) C, (c) Fe, and (d) W of Fe_3C/WC/GC composite.

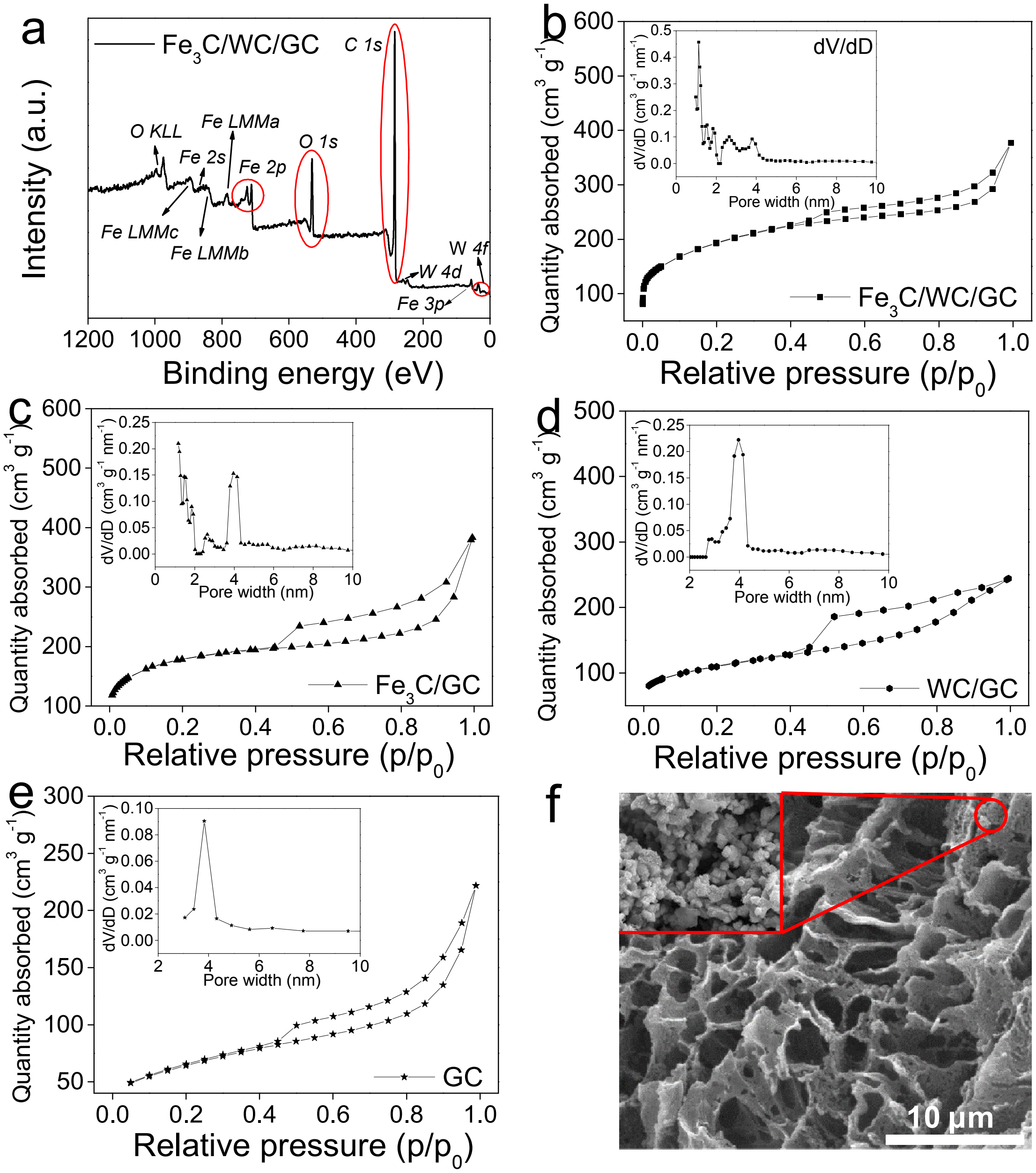

Figure S3. (a) XPS overview spectrum of $Fe_3C/WC/GC$ carbonized at 1000 °C, (b–e) N_2 adsorption/desorption isotherms and pore size distributions curves of $Fe_3C/WC/GC$, Fe_3C/GC, WC/GC, and GC, respectively, (f) SEM image of $Fe_3C/WC/GC$ after acid leaching.

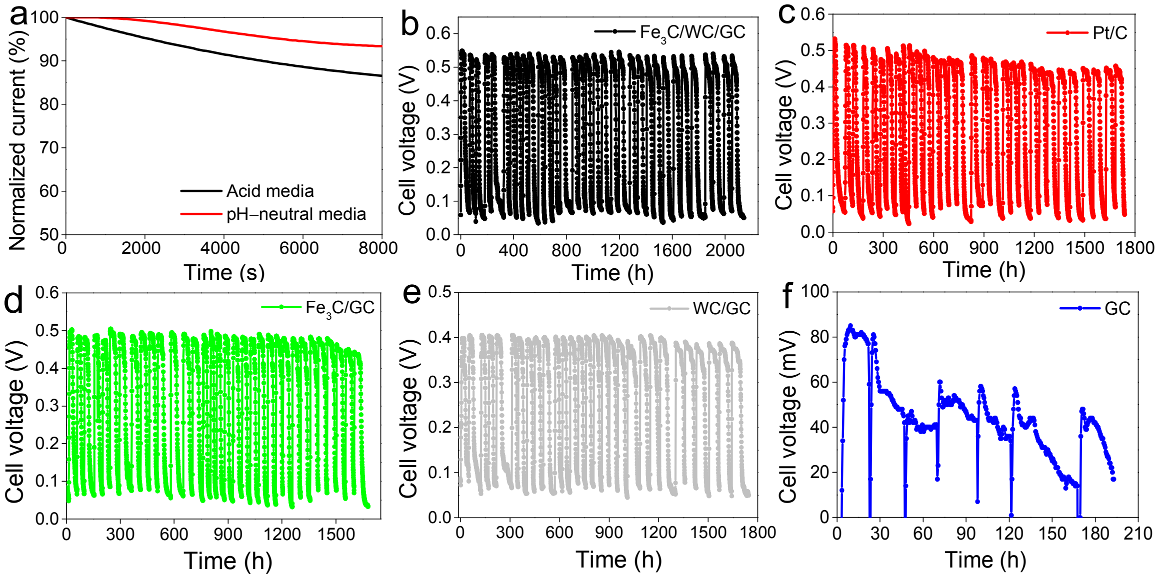

Figure S4. (a) Durability of Fe_3C/WC/GC catalyst in pH–neutral media and acid media, (b–f) voltage output of Fe_3C/WC/GC, Pt/C, Fe_3C/GC, WC/GC, and GC, respectively.

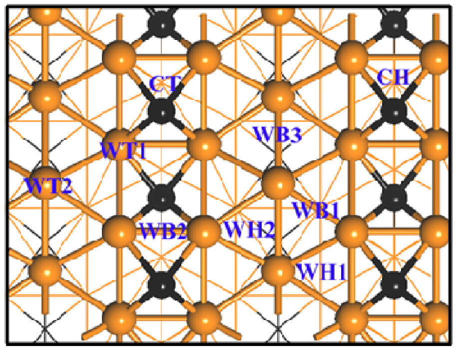

Figure S5. Structures and possible oxygen adsorption sites on $Fe_3C(001)$ surface: C–top (CT), C–hollow (CH), W–top (WT1 and WT2), W–bridge (WB1, WB2 and WB3), and W–hollow (WH1 and WH2). The orange balls for Fe atoms, black balls for the surface layer C atoms.

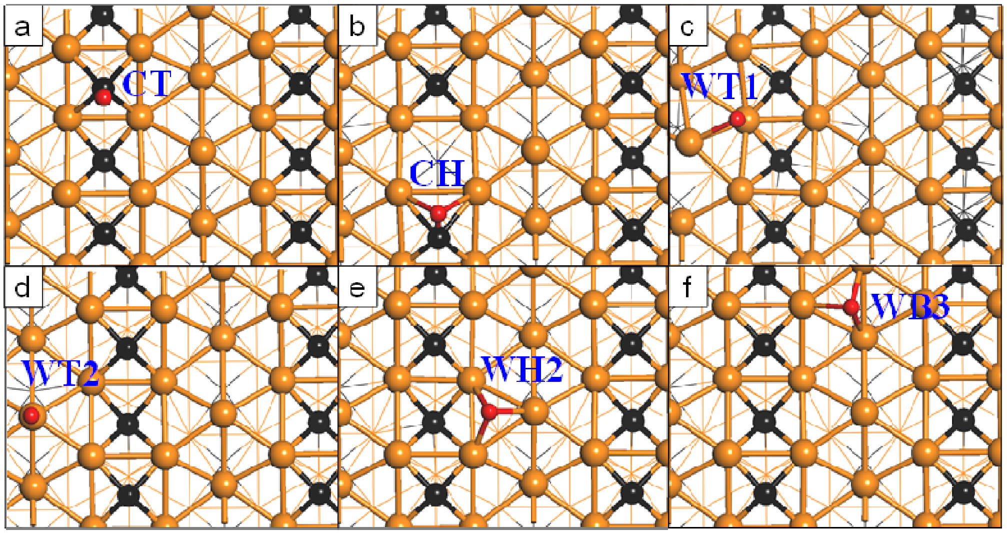

Figure S6. The relaxed stable structures of atomic oxygen (the red balls) adsorption on $Fe_3C(001)$ surface. With all the possible adsorption sites shown in Figure S1, only six adsorption structures are stable after full relaxation, which are (a) CT, (b) CH, (c) WT1, (d) WT2, (e) WH1 and (f) WH2.

Table S1. Electrochemical impedance fitting results and maximum power density of different cathodes.

	R_o (Ω)	R_{ct} (Ω)	P_{max} (mW m^{-2})
Fe_3C/WC/GC	0.216	144.4±5.1	1997±13
Pt/C	0.231	154.4±4.3	1190±37
Fe_3C/GC	0.218	147.5±6.8	1605±24
WC/GC	0.243	163.5±4.4	799±35
GC	0.206	182.3±3.8	71±5

Table S2. Koutecky−Levich results for different catalysts.

	Fit linear equation	R^2	Electron transfer number
Fe_3C/WC/GC	y=0.237x+0.5013	0.9999	3.95
Pt/C	y=3.2063x+0.5	0.9998	3.59
Fe_3C/GC	y=2.017x+0.5197	0.9999	3.74
WC/GC	y=4.0205x+1.0362	0.9997	2.86
GC	y=7.3795x+1.8196	0.9998	1.87

Table S3. Researches with excellent performances reported in microbial fuel cells area.

Catalyst	Morphology	Electrolyte (PBS, mM)	OCV (V)	Power density (mW m^{-2})	Electron transfer number	Ref.
Fe/Fe_3C−C	Nanorod	100	0.82	472.5	3.98	[16]
Fe−N−GE		50		1149.8		[68]
Co/Fe−PDAP	Nanosphere	50	0.7 ± 0.01	1100 ± 0.01		[69]
MnO_2−NTs	Nanotube	50	0.812	1872		[70]
N−CNTs	Bamboo−like	50	0.59	1600 ±50		[71]
Pt−CNT−textile	Nanowire	100		837		[72]

Table S4. The adsorption energy (E_{ads}) of atomic oxygen on $Fe_3C(001)$.

Site	CT	CH	WT1	WT2	WH1	WH2
E_{ads} (eV)	1.630	1.654	0.275	1.424	2.434	2.891